Appendix 1

Algorithm of two-pass phase-shift migration

First pass of conventional downward extrapolation

2-D Fourier transform of stacked section: $P(t, x, \tau{=}0) \rightarrow P(\omega, k_x)$

For each step $\tau = \Delta\tau, 2\Delta\tau, \ldots, \tau_{\max}$:

{

For all k_x :

{

Normal Image: $N(k_x, \tau) = 0$

For $|\omega| > |k_x| v$:

{

$P(\omega, k_x) = P(\omega, k_x) \times \exp[-i\,\omega\Delta\tau \sqrt{1-(vk_x/\omega)^2}]$

$N(k_x, \tau) = N(k_x, \tau) + P(\omega, k_x)$

}

}

1-D inverse Fourier transform : $N(k_x, \tau) \rightarrow N(x, \tau)$

}

Second pass of upward extrapolation

For each step $\tau = \tau_{\max}, \tau_{\max}-\Delta\tau, \ldots, \Delta\tau$:

{

For all k_x :

{

Overturned Image: $O(k_x, \tau) = 0$

For $|k_x| v \leq |\omega| < |k_x| v_{\max}$:

{

$P(\omega, k_x) = P(\omega, k_x) \times \exp[-i\,\omega\Delta\tau \sqrt{1-(vk_x/\omega)^2}]$

$O(k_x, \tau) = O(k_x, \tau) + P(\omega, k_x)$

}

}

1-D inverse Fourier transform : $O(k_x, \tau) \rightarrow O(x, \tau)$

}

Appendix 2

Ray tracing in constant-velocity-gradient media

In a medium with a constant velocity gradient, i.e., velocity defined by

$$v(z) = v_0(1 + \beta z), \tag{A-2-1}$$

rays travel along circular arcs (Slotnick, 1959). Figure A-2.1 shows the geometry of a nonzero-offset recording. Normal reflections are obtained when the reflector angle α is from 0 to 90 degrees, while overturned reflection modeling corresponds to an α between 90 and 180 degrees. The propagating angle θ of a ray is defined as the angle between the ray's direction and the vertical axis. This angle θ is between -180 and +180 degrees, and is positive when the ray travels to the right, negative when the ray travels to the left.

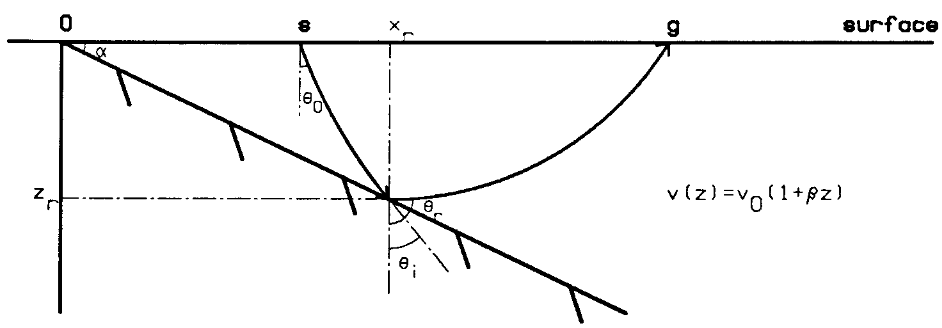

FIG. A-2.1. A nonzero-offset recording geometry. The angle θ_i is the propagating angle of the incident ray at the reflector, while θ_r is the propagating angle of the reflecting ray at the reflector.

The underground position (x, z) through which a particular ray, with a given initial take-off angle θ_0, passes, and the arrival time of the ray at (x, z) follow (Li et al., 1984):

$$\begin{cases} x = s + \dfrac{1}{v_0\beta p}\left[\sqrt{1-p^2v_0^2} - \sqrt{1-p^2v^2(z)}\right], \text{ and} \\ t = \dfrac{1}{v_0\beta}\ln\left(\dfrac{(1+\beta z)\left[1+\sqrt{1-p^2v_0^2}\right]}{\left[1+\sqrt{1-p^2v^2(z)}\right]}\right), \end{cases} \tag{A-2-2}$$

and

$$\begin{cases} x = s + \dfrac{1}{v_0\beta p}\left[\sqrt{1-p^2v_0^2} + \sqrt{1-p^2v^2(z)}\right], \text{ and} \\ t = \dfrac{1}{v_0\beta}\ln\left(\dfrac{\left[1+\sqrt{1-p^2v_0^2}\right]\left[1+\sqrt{1-p^2v^2(z)}\right]}{p^2v_0v(z)}\right), \end{cases} \tag{A-2-3}$$

where $p = \sin\theta/v(z) = \sin\theta_0/v_0$ is the ray parameter, and s is the source position on the x axis. Equation (A-2-2) is used if the ray reaches (x, z) before it turns around at its turning point (Li et al., 1984); otherwise equation (A-2-3) should be used.

The reflector's position (x_r, z_r) corresponding to a given ray parameter $p = \sin\theta_0/v_0$ is obtained by solving the following system of equations:

$$\begin{cases} x_r = s + \dfrac{1}{v_0\beta p}\left[\sqrt{1-p^2v_0^2} \pm \sqrt{1-p^2v_0^2(1+\beta z_r)^2}\right], \text{ and} \\ x_r = \dfrac{z_r}{\tan\alpha}. \end{cases} \tag{A-2-4}$$

The propagating angle of the reflecting ray at (x_r, z_r) is given by

$$\theta_r = 180^o - 2\alpha - \theta_i, \tag{A-2-5}$$

where θ_i can be determined by $\sin\theta_i = v(x_r, z_r)\sin\theta_0/v_0$.

Having determined θ_r, we obtain the ray parameter for the reflecting ray. Thus, the receiver position and the travel time for the reflecting ray can be calculated by equation (A-2-2) or (A-2-3), depending on whether the propagating angle of the ray at the reflector position is larger or smaller than 90 degrees.

Figures A-2.2 and A-2.3 show recording geometries and travel-time curves for a normal reflection and an overturned reflection, respectively. The ray-tracing results show that time-distance curves for normal reflections and overturned reflections have opposite curvatures in common-shot gathers. The travel-time curve for the normal reflection has a positive second derivative, while that for the overturned reflection is negative.

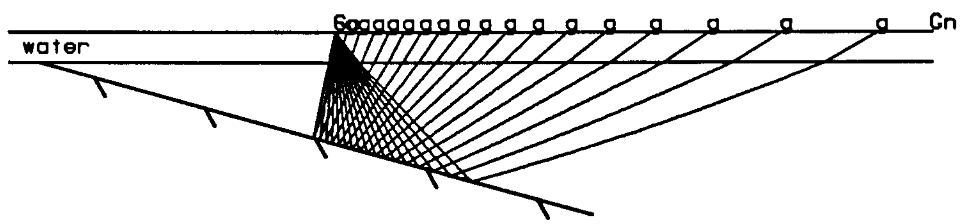

a

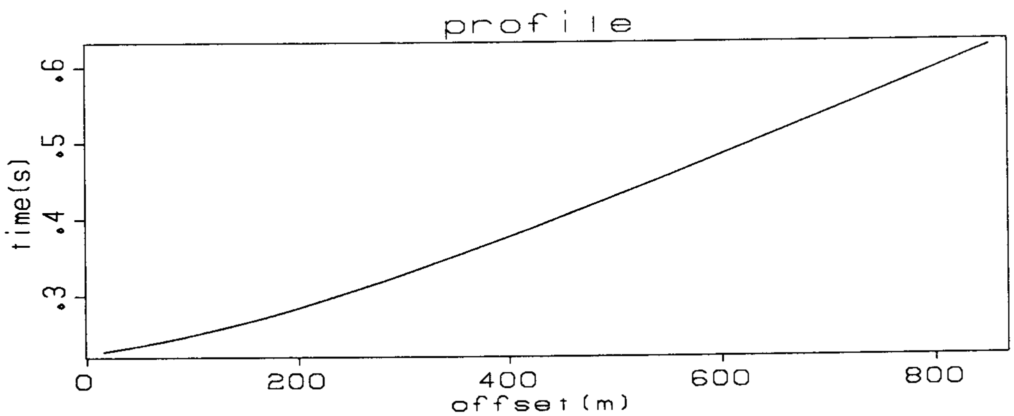

b

FIG. A-2.2. **a.** Recording geometry for normal reflections. The dip of the reflector α is 15 degrees. The water depth is 50 m and the water velocity is 1500 m/s. The sediment velocity is given by $v(z) = 1600(1+.0002z)$; the shot position is $s = 500$ m; and the cable length is 1000 m. **b.** Travel-time curve of the normal reflections. The curve has positive second derivatives, or curvatures.

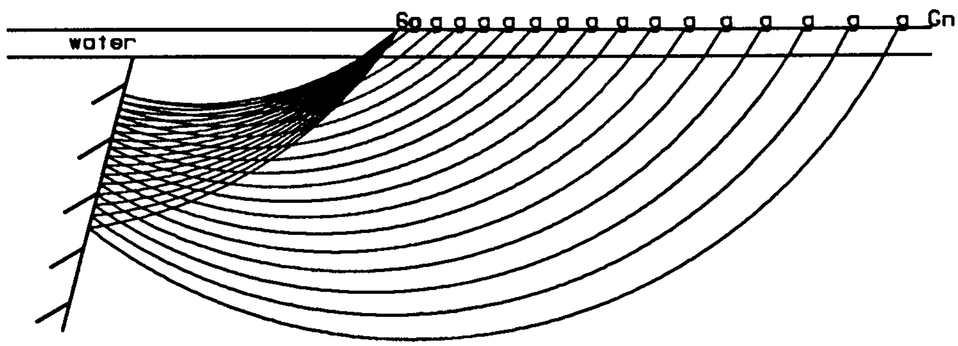

a

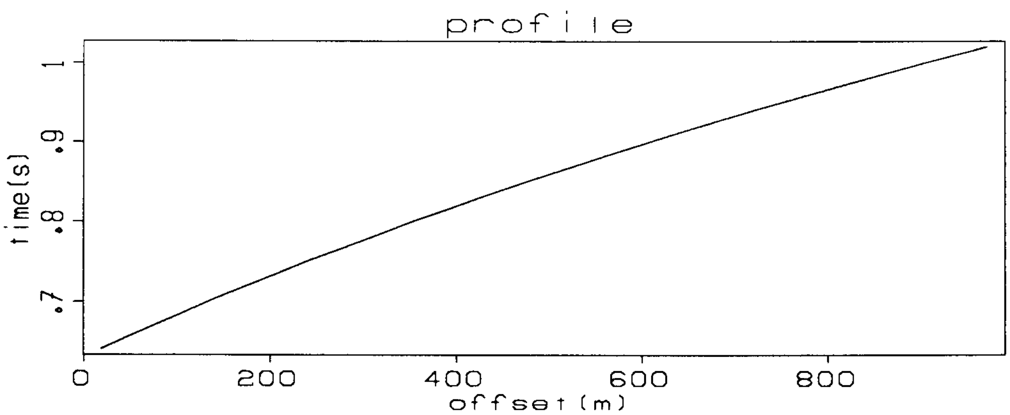

b

FIG. A-2.3. **a.** Recording geometry for overturned reflections. The dip of the reflector α is 105 degrees. The water depth is 50 m and the water velocity is 1500 m/sec. The sediment velocity is given by $v(z) = 1600(1+.002z)$; the shot position is $s = 500$ m; and the cable length is 1000 m. **b.** Travel-time curve of the normal reflections. The curve has negative second derivatives, or curvatures.

The seismograms generated by the ray-tracing algorithm just described are calculated after scanning over some initial angles, θ_0's. The time-distance curve is not evenly sampled over the horizontal axis (the geophone axis g). To obtain a common-midpoint gather, interpolation (e.g., spline interpolation) is necessary. Figure A-2.4 shows the common-midpoint gathers for normal reflections and overturned reflections. Opposite moveouts for normal and overturned reflections can be seen in the figure. The travel times of the overturned reflections in a common-midpoint gather decrease as the offsets increase!

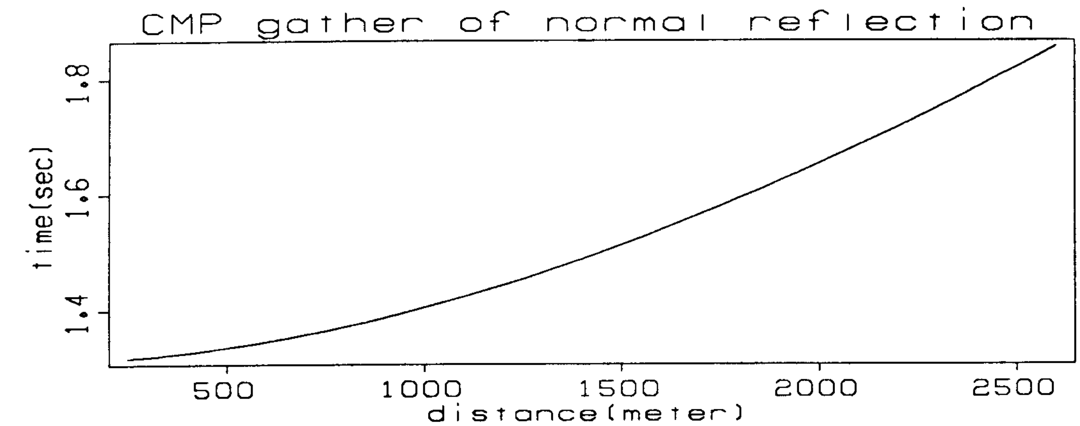

a

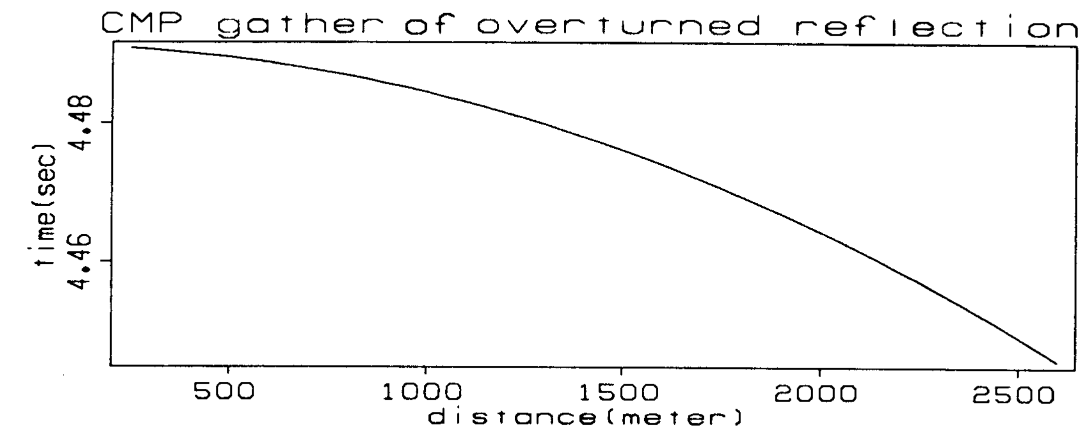

b

FIG. A-2.4. **a.** Common-midpoint gather for normal reflections. **b.** Common-midpoint gather for overturned reflections.

Appendix 3

Accuracy and stability of the 1-D characteristic method

The one-dimensional upcoming wave equation can be written as

$$\frac{\partial P}{\partial z} - \frac{1}{v}\frac{\partial P}{\partial t} = 0 , \qquad \text{(A-3-1)}$$

where v is velocity, z depth, and t time.

The leap-frog finite-difference approximation to equation (A-3-1) is

$$P(t_n + \Delta t , z_j) = P(t_n - \Delta t , z_j) + \lambda v \left[P(t_n , z_j + \Delta z) - P(t_n , z_j - \Delta z) \right] , \qquad \text{(A-3-2)}$$

where $\lambda = \Delta t / \Delta z$. This method is stable when $\lambda \leq 1$ and is accurate to the second orders of Δt and Δz (Mitchell and Griffiths, 1980).

Applying the characteristic coordinate transformation

$$\begin{cases} \xi = t + z/v \\ \eta = t - z/v \end{cases} , \qquad \text{(A-3-3)}$$

equation (A-3-1) can be transformed to

$$\frac{\partial P}{\partial \eta} = 0 , \qquad \text{(A-3-4)}$$

The finite-difference method is then

$$P(\eta_n) = P(\eta_n - \Delta\eta) = P(\eta_0) . \qquad \text{(A-3-5)}$$

Clearly, the finite-difference solution of the characteristic equation is exact and unconditionally stable.

References

Baysal, E., Kosloff, D.D., and Sherwood, J.W.C., 1984, A two-way nonreflecting wave equation: Geophysics, **49,** 132-141.

Berg, P.W., and McGregor, J.L., 1966, Elementary partial differential equations: Holden-Day.

Botha, J.F., and Pinder, G.F., 1983, Fundamental concepts in the numerical solution of differential equations: John Wiley & Sons.

Claerbout, J. F., 1976, Fundamentals of geophysical data processing: McGraw-Hill.

Claerbout, J. F., 1985, Imaging the earth's interior: Blackwell Scientific Publications.

Dix, C.H., 1955, Seismic velocities from surface measurements: Geophysics, **20,** 68-86.

Engquist, B. and Majda, A., 1977, Absorbing boundary conditions for the numerical simulation of waves: Mathematics of Computation, **31, 139,** 629-651.

Fowler, P., 1984, Velocity independent imaging of seismic reflectors: Presented at the 54th Annual International SEG Meeting in Atlanta.

Gazdag, J., 1978, Wave equation migration with the phase shift method: Geophysics, **43,** 1342-1351.

Gazdag, J. and Sguazzero, P., 1984, Migration of seismic data by phase shift plus interpolation: Geophysics, **49,** 124-131.

Hale D., 1983, Dip-moveout by Fourier transform: Ph.D. thesis, Geophysics Department, Stanford.

Hatton, L., Larner, K., and Gibson, B.S., 1981, Migration of seismic data from inhomogeneous media: Geophysics, **46,** 751-767.

Jacobs A., 1982, The pre-stack migration of profiles: Ph.D. thesis, Geophysics Department, Stanford.

Judson, D.R., Schultz, P.S., and Sherwood, J.W.C., 1978, Equalizing the stacking velocities of dipping events via Devilish: Presented at the 48th Annual International SEG Meeting in San Francisco.

Judson, D.R., Lin, J., Schultz, P.S., and Sherwood, J.W.C., 1980, Depth migration after stack: Geophysics, **45,** 361-375.

Levin, F.K., 1971, Apparent velocity from dipping interface reflections: Geophysics, **36,** 510-516.

Li, Z., Claerbout, J. F. and Ottolini, R., 1984, Migrating reflections greater than 90 degrees via depth extrapolation: SEG Expanded Abstracts with Biographies of 1984 Technical Program, 696-700.

Loewenthal, D., Lu, L., Roberson, R. and Sherwood, J., 1976, The wave equation applied to migration: Geophysical Prospecting, **24,** 380-399.

Ma, Z., 1982, Finite difference migration with higher order approximation: Oil Geophysical Prospecting, China, **1,** 6-15.

Mayne, W.H., 1962, Common reflection point horizontal data stacking techniques: Geophysics, **27,** 927-938.

Mitchell, A., and Griffiths, D., 1980, The finite-difference methods in partial differential equations: John Wiley & Sons.

Slotnick, M.M., 1959, Lessons in seismic computing: Wisconsin, George Banta Company.

Stolt, R., 1978, Migration by Fourier transform: Geophysics, **43,** 23-48.

Toldi, J., 1985, Velocity analysis without picking: Ph.D. thesis, Geophysics Department, Stanford.